TAO, Vol. 16, No. 1, 19-44, March 2005

Core Description and a Preliminarily Sedimentology Study of Site 1202D, Leg 195, in the Southern Okinawa Trough

Chi-Yue Huang[1,*], Ya-Ling Chiu[1], and Meixun Zhao[1,2]

(Manuscript received 15 August 2004, in final form 8 November 2004)

ABSTRACT

ODP Site 1202 of Leg 195 was designed primarily for a high-resolution study of the paleoceanography of the Kuroshio Current in the southern Okinawa Trough off NE Taiwan. Four holes were drilled in which Hole 1202D is described in detail in this study for an assessment of core quality for paleoceanography study and understanding of sedimentological features, especially turbidite sedimentation and the sediment provenances during the Late Quaternary in the southern Okinawa Trough. Pelagic mud with insignificant silt or sand layers is observed from the core top down to 133 m (mbsf; Marine Isotope Stages 1-3), but the silt-sand layer ratio (SLR: total thickness of silt and sand layers / 1.5 m of core) increases gradually from a value of < 10 % between 133 and 167 m to values > 50 % between 223 and 279 m, followed by decreases to values <10 % between 310 and 337 m and to < 3 % between 337 and 407 m (Stage 4). These silt-sand layers were most likely derived by fine-grained turbidite gravity flows, which were very active during Stages 3 and 4. Slate fragments, quartz grains, mica flakes and volcanic detritus are the major components in the coarse fraction of wash residues (> 250 μm). Slate fragments are commonly found in fine-grained turbidite dominant intervals (160 - 280 m), while mica flakes can be observed in the muds throughout the core. The major detrital components were derived primarily from the Miocene slate belt of the pre-collision accretionary prism of the Central Range in northern Taiwan. The occurrence of volcanics could represent submarine volcanic activity in the active-opening Okinawa Trough back-arc basin off NE Taiwan. Shallow-marine fossils including benthic foraminifers, echinoids, bryozoans and mollusks are also found in the fine-grained turbidite dominant intervals. These fossil

[1] Department of Earth Sciences, National Cheng Kung University, Tainan, Taiwan, ROC

[2] Department of Earth Sciences, Dartmouth College, Hanover, USA

* *Corresponding author address:* Prof. Chi-Yue Huang, Department of Earth Sciences, National Cheng Kung University, Tainan, Taiwan, ROC; E-mail: huangcy@mail.ncku.edu.tw

assemblages could have been deposited in the shallow shelf and then transported to the depositional site along with voluminous terrigenous materials derived from Taiwan, via submarine channels or by slope failures due to frequent earthquakes induced by plate convergence/collision and extension in the southwestern Okinawa Trough off NE Taiwan. It is concluded that the top 133 m of the core is better suited for paleoceanographic reconstruction.

(Key words: Okinawa Trough, Turbidite sedimentation, Central Range, Taiwan, Paleoceanography)

1. INTRODUCTION

Site 1202 (24°48.24'N, 122°30.00'E, water depth 1274 m), Leg 195, was designed for a high-resolution paleoceanographic study of the Kuroshio Current in the Western Pacific (Shipboard Scientific Party, 2002). The site is located near the southwestern tip of the active-opening back-arc basin Okinawa Trough off NE Taiwan (Fig. 1). More than 800 meters of deep-sea sediments in 4 holes were drilled (Holes 1202A, B, C, and D). Hole A, Hole B, Hole C and the upper part of Hole D were recovered by using APC core; while the lower part of Hole 1202D was drilled using XCB coring method (Shipboard Scientific Party 2002). Magnetic susceptibility of the four holes was measured on board *JOIDES Resolution* providing an independent physical property for core correlation. However, most cores were not described in details onboard because of the short time interval before *R/V JOIDES Resolution* arriving at the next site of Leg 196. Therefore, the purposes of this paper are to present the core description of Hole D, the longest record of the four holes, and give preliminary results for the sedimentological study of the silt-sand layers and their detritus compositions in the coarse fraction of wash residues (> 250 μm) for better evaluation of core quality in preparation for a high-resolution study of the paleoceanography of the Kuroshio Current (Wei et al. 2005; Zhao et al. 2005).

2. METHODS

The working half of Hole 1202D was examined for this description under stereomicroscope (X60-120) at TAMU core lab. The description focuses on occurrence of silt and sand layers in the sequence. Notes were carefully taken on any visible turbidite structures, such as grain size, grading, basal erosion, cross-ripples, detritus compositions, and fossil remains. Silt-sand ratio (SLR) in each 1.5 m section of core is calculated for an evaluation of core quality for paleoceanographic study and for a better understanding of their depositional mechanisms. Terrigenous detritus in wash residues (> 250 μm) in 120 samples (average of sampling interval: 3.4 m) were also determined under stereo-microscope (X60) for evaluating the source of sediments. An age model based on oxygen isotope stratigraphy and AMS ^{14}C dating by Wei et al. (2005) was followed.

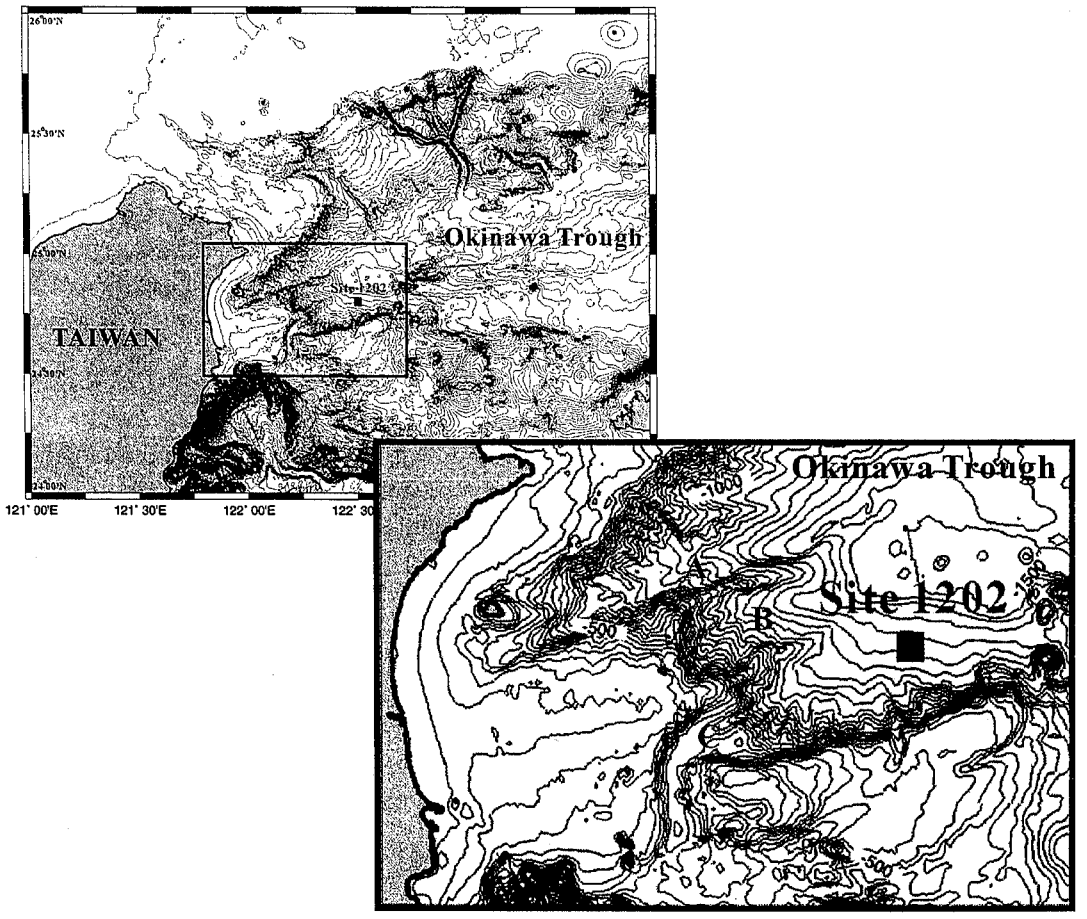

Fig. 1. Site location of Hole 1202D, Leg 195, in the southern Okinawa Trough off NE Taiwan.

3. RESULTS

3.1. Core Description

Description of each section of core is printed in this volume. The sedimentary feature details of each section can be found in the appendix.

3.1.1 Cores 1-3 (0 - 19.2 mbsf)

Cores 1-3 are exclusively of hemipelagic mud without any visible silt-sand layer (Appendix Fig. 1).

3.1.2 Core 4 (19.2 - 29.38 mbsf)

Core 4 is composed of hemipelagic mud with insignificant thin layers of very fine sand and silt (Appendix Fig. 2). A fine sand layer in 37 - 39 cm of section 1, associated with echinoid spines and plates, foraminifers and slate chips could be correlated with a fine sand layer in 87 - 90 cm of section 1, Core 4 of Hole 1202B. Above this key bed, there is no silt-sand layer in either Hole 1202B or Hole 1202D. Three graded fine sand layers and wood remains, echinoid plates and a gastropod can be observed in section 3. Bivalve fragments with slates in a thin fine sand layer (83.4 - 84.6 cm, section 5) provide another key interval for a correlation between core 4 of Hole 1202D and a fine sand layer (70 - 71.5 cm section 4), Core 4 of Hole 1202B. Small scaphopods *Dentalium* shells are commonly found in mud intervals of section 6.

3.1.3 Core 5 (28.7 - 38.5 mbsf)

Core 5 is primarily composed of hemipelagic mud with insignificant turbidite sand layers in sections 1, 2 and 4 (Appendix Fig. 3). Basal erosion and grading features are observed in these turbidite layers in which slate chips, mica flakes and quartz grains are commonly found. Very fine sand layers occur more frequently in the lower part (sections 6, 7 and core CC) of Core 5.

3.1.4 Core 6 (38.2 - 48.63 mbsf)

Core 6 is predominated by hemipelagic mud with some very thin layers (< 0.1 cm) of whitish silt to very fine sand (Appendix Fig. 4). Quartz grains are commonly found in these very fine sand layers. Slate chips are rather abundant in a fine sand layer (78.2 - 79.4 cm) of section 4.

3.1.5 Core 7 (47.7 - 58.14 mbsf) and Core 8 (57.2 - 67.5 mbsf)

The lithology of Core 7 (Appendix Fig. 5) and Core 8 (Appendix Fig. 6) is very similar to Core 6 in which some very fine sand layers (each < 0.1 cm) intercalate within hemipelagic mud. The remains of some wood can be observed at 48 cm in section 3 of Core 7.

3.1.6 Core 9 (66.7 - 77.04 m)

Core 9 is almost exclusively of hemipelagic muds (Appendix Fig. 7).

3.1.7. Core 10 (76.2 - 79.74 mbsf)

Core 10 (Appendix Fig. 8) is generally composed of mud with three layers of very fine sand in section 1 and a pumice layer for 3 cm (34 - 37 cm) in section 3. Some isolated pumice grains are also observed in section 3. The occurrence of these pumice layers and grains provides a key marker for correlation with section 5 in core 10 of Hole 1202B (Appendix Fig. 8).

(Key words: Calcareous nannofossils, ODP Hole 1202B, Kuroshio Current, Pleistocene and Holocene)

1. INTRODUCTION

The Kuroshio (Black Current) is the biggest western boundary surface current in the western Pacific. It plays an important role in transporting heat, mass, momentum, and moisture from the western Pacific warm pool to high latitudes in the North Pacific. The Kuroshio Current is characterized by its high temperature and salinity (Fan 1985; Yuan et al. 1998). The present Kuroshio Current passes between Taiwan and the southernmost part of the Ryukyu Island arc and then flows northeastward along the area between the trough and the outer edge of the East China Sea continental shelf (Fig. 1 and Fig. 2).

A number of previous study suggested that the Okinawa Trough changed from an open-sea environment to a semi-enclosed marginal basin during the last glacial maximum (LGM, occured around 25 - 16 kaBP with coldest period at 21 kaBP), because of a 120-m sea level drop (Fairbanks 1989) and the emergence of a Ryukyu-Taiwan land bridge, which was suggested by Ujiié and Ujiié (1999) with a number of evidences. The Ryukyu-Taiwan land bridge prevented the Kuroshio Current from entering into the Okinawa Trough, as a result, the Kuroshio Current turned to the east at the southern end of the Ryukyu arc (Ujiié et al. 1991, Ujiié and Ujiié 1999) (Fig. 2). The inference made in the previous studies about the course changes of the Kuroshio Current was mainly based on plankton foraminiferal assemblages and $\delta^{18}O$ data. Results of these studies regard *Pulleniatina obliquiloculata* as a good and sensitive indicator of the presence of the Kuroshio Current and high percentages of this species are restricted to the main route of the Kuroshio Current (Ujiié and Ujiié 1999, Jian et al. 2000).

In 2001, JOIDES Resolution of the Ocean Drilling Program sailed into Okinawa Trough, and drilled Site 1202 on the southern slope of the Okinawa Trough. One of the major paleoceanographic objectives for this Site is to obtain a high-resolution record about the history of the Kuroshio Current during the Quaternary.

Calcareous nannofossils from sediments of Hole 1202B were studied to obtain a high-resolution nannofossil record of the change of the Kuroshio Current during the last glacial and the Holocene.

2. MATERIALS AND METHODS

2.1 Materials

Surface Samples

Sea floor surface sediments under the recent Kuroshio Current and its adjacent areas in the East China Sea were collected and studied.

A total of 14 surface sediment samples in 4 west-east transects extending from the East China Sea continental shelf to the Okinawa Trough from north to south were analyzed (Fig. 1).

the continental shelf are very common in sand layers of section 2. Some shallow-marine benthic foraminiferal tests even show black in color suggesting that they were eroded from the old strata of continental shelf environments. The coarse part of sediment (> 250 μm) is predominated by slate chips and bioclastics with rare schist and mica flakes.

3.1.14 Core 17 (143.4 - 152.74 mbsf)

The number and thickness of turbidite sand layers in Core 17 (Appendix Fig. 15) are more than those of Core 16 (Appendix Fig. 14). Basal erosion, grading and the presence of shallow-marine fauna indicate frequent turbidite sedimentation. Particles of several thicker sand layers (> 3 cm) may reach fine to medium grain size. Coarse fraction (>250 μm) of wash residues is predominated by slate chips and quartz with minor schist and mica flakes. Bioclastics of mollusks, bryozoans, echinoid spines, spongy spicules and benthic foraminifers derived from shallow-marine environments are very common. Planktic foraminifers are rather abundant in turbidite sand layers (e.g., 11-16 cm of section 4) presumably due to turbidite sorting. In contrast, in hemipelagic mud between turbidite sand layers both benthic and planktic foraminifer are rare (e.g., 58 - 63 cm of section 4 and 63.5 - 68 cm of section 6).

3.1.15 Core 18 (153.0 - 161.75 mbsf)

In Core 18 (Appendix Fig. 16) turbidite sand layers are common with abundant slate chips and displaced shallow-marine benthic foraminifers. In the turbidite sands, some foraminifers (both benthics and planktics) show black in color, suggesting they were reworked from the older strata of shelf deposits by turbidite erosions. However, foraminifers are very rare in hemipelagic mud (113 - 118 cm of section 1, 64 - 67 cm of section 4 and 63 - 68 cm of section 1), similar to what is observed in Core 17.

3.1.16 Core 19 (162.7 - 171.17 mbsf)

Core 19 is a hemipelagic mud dominant interval (Appendix Fig. 17). The number of sand layers in Core 19 is much less than in Cores 20 and 18. In these hemipelagic mud intervals, there are almost no displaced shallow-marine fauna. However, planktic and indigenous benthic foraminifers are also rare due to a high sedimentation rate.

3.1.17 Core 20 (172.3 - 180.15 mbsf)

Core 20 is characterized by the occurrence of turbidite sand layers, especially in the lower part (sections 3 - 5, Appendix Fig. 18). Basal erosion and grading feature from fine sand upward to silt and mud are commonly observed in each of the turbidite sand layers in which planktic foraminifers are abundant (e.g., 100 - 105 cm of section 4), but slate chips and mica flakes are rare. Bioclastics of echinoid spines and thin-shell bivalves are also rich in the turbidite sands.

3.1.18 Core 21 (172.3 - 180.15 mbsf)

The number and thickness of sand layers increase form Core 21 to Core 31. Core 21 (Appendix Fig.19) is characterized by the occurrence of rich foraminifers tests, molluscan fragments and echinoid spines with abundant slate chips in thick sand layers (> 5 cm, e.g., at 38 - 43 cm and 99 - 104 cm of section 2), while bioclastics, foraminifers and slate chips are rare, but mica flakes are abundant in the thin sand layers (< 5 cm; e.g., at 21.2 - 25.6 cm of section 1; 103 - 108 cm and 125 - 130 cm of section 3). Distinct sorting effects caused by stronger turbidity flows would have resulted in the deposition of thick turbidite sand layers and the common occurrence of continent-derived slate chips and displaced shallow-marine bioclastics.

3.1.19 Core 22 (191.7 - 199.73 mbsf)

Grading features are commonly found in the turbidite sand layers of Core 22 (Appendix Fig. 20). Pumice grains and slate chips along with mica or schist flakes are found in 95 - 98 cm of section 1. In hemipelagic mud, continent-derived detritus and foraminifers are rare (114-118 cm and 125 - 130 cm of section 3), while in turbidite sand layers (e.g., at 95 - 98 cm of section 1 and 32 - 36 cm of section 4) displaced benthic foraminifers, echinoid spines and molluscan fragments of shallow-marine fauna are common.

3.1.20 Core 23 (201.3 - 208.5 mbsf)

Core 23 contains many turbidite sand layers (Appendix Fig. 21). Some of them may reach 5-8 cm in thickness of which basal erosion and grading features are common. Most of the sand layers contain rich slate fragments. However, volcanic detritus and minerals with well-crystallized forms along with slate chips and quartz grains can be observed in the fine sands of section 5 (108 - 110 cm). Again as with the other cores, abundant shallow-marine benthic foraminifers, molluscan fragments and echinoid plates and spines can be found in the thick turbidite sands (138 - 143 cm of section 3), but they are rare in hemipelagic mud. Instead, indigenous benthic foraminifers are predominant in hemipelagic muds (125 - 130 cm of section 3)

3.1.21 Core 24 (210.9 - 219.13 mbsf)

Turbidite sand layers are commonly observed in Core 24 (Appendix Fig. 22). Volcanic detritus and minerals with well-developed crystal forms are found in 74 - 77 cm, section 5. Displaced shallow-marine benthic foraminifers, molluscan fragments and echinoid spines are abundant in the thick turbidite sand layers (74 - 77 cm, section 5).

3.1.22 Core 25 (220.5 - 224.31 mbsf)

A large part of Core 25 (Appendix Fig. 23) was not recovered by XBC coring probably due to the predominance of sand layers. Volcanic detritus can be found in 63 - 67 cm of section

2 with very rare foraminifers. However, slate chips are abundant in the bottom of core CC.

3.1.23 Core 26 (230.1 - 230.3 mbsf)

Core 26 was almost un-recovered (Appendix Fig. 24). Fine sands without foraminifers, but with abundant mica flakes and organic materials (grass?), can be observed in core CC.

3.1.24 Core 27 (239.7 - 244.0 mbsf)

Core 27 is dominated by turbidite sand layers with normal grading structures and basal erosions (Appendix Fig. 25). Fauna are very rare in either the hemipelagic mud or turbidite sand layers. If there are benthic foraminifers, they are all shallow-marine species displaced from shallow-marine environments. However, organic materials and mica flakes are found in some fine sand layers (for example, 113 - 116 cm, section 3).

3.1.25 Core 28 (249.3 - 253.29 mbsf)

Core 28 is composed predominantly of turbidite fine-grain sands with grading structures (Appendix Fig. 26). Each turbidite sand layer may reach 15 cm in thickness. Samples ranging from very fine sand to the silt part of the turbidite layer (125 - 130 cm, section2; 70 - 75 cm of section 3) contain very rich mica flakes and quartz grains, presumably derived from the Central Range of Taiwan. Organic materials, presumably plant, are abundant, suggesting the deposition site was not far from land. Microfossils foraminifers are very rare.

3.1.26. Core 29 (nothing recovered)

Nothing was recovered from Core 29.

3.1.27 Core 30 (268.5 - 270.54 mbsf)

Only a small portion of Core 30 was recovered (Appendix Fig. 27). Core 30 is predominated by turbidite sands with grading structures. Foraminifers range from rare to common. Most of them were displaced from a shallow-marine environment. Mica flakes are very abundant.

3.1.28 Core 31 (279.6 - 286.47 mbsf)

The number of sand layers decreases from Core 31 (Appendix Fig. 28) downward. Although turbidite sand layers are fewer than in Cores 30 - 20, foraminifers in either hemipelagic mud (80 - 85 cm, section 2) or turbidite sands (80 - 85 cm of section 3; 15.0 - 15.2 cm of section 5; 24 - 34 cm and 54 - 59 cm of section 6) are predominated by displaced shallow-marine species. Volcanic pumice and volcanic minerals with well-developed crystal forms can be observed in 80 - 85 cm of section 4 and 24 - 27 cm, 27 - 34 cm, 54 - 59 cm of section 6. Slate chips are also found in some sand layers (e.g., at 80 - 85 cm of section 4).

3.1.29 Core 32 (287.8 - 295.15 mbsf)

Core 32 (Appendix Fig. 29) contains more sand layers than in Core 31 (Appendix Fig. 28). Volcanic detritus are commonly found in the lower part (58 - 69 cm of section 4 and 9 - 14 cm, 114 - 121 cm of sections 5). Foraminifers are rare in the turbidite sand layers.

3.1.30 Core 33 (297.4 - 305.93 mbsf)

Core 33 is composed predominantly of hemipelagic mud with several very fine sand layers (Appendix Fig. 30). Detritus of coarse fraction are rare, but mica and slate are found. Foraminifers are almost barren in either hemipelagic mud or sand layers indicating a high sedimentation rate.

3.1.31 Core 34 (307.0 - 315.57 mbsf)

Core 34 consists predominantly of hemipelagic mud (Appendix Fig. 31). Turbidite sands with volcanic detritus can be found in 25 - 39 cm of section 2, 105 - 109 cm of section 3, and 55 - 59 cm of section 4. Foraminifers are rare but benthic species are all indigenous. Mica flakes can be found in the hemipelagic mud.

3.1.32 Core 35 (316.6 - 325.29 mbsf)

Core 35 is composed of hemipelagic mud with some silt to very fine sand layers (Appendix Fig. 32). Due to a high sedimentation rate, microfossils are all very rare in the sediments. Volcanic detritus are frequently found in sections 3, 4 and 5.

3.1.32 Core 36 (326.2 - 335.9 mbsf)

Core 36 (Appendix Fig. 33) is predominated by hemipelagic mud almost without any visible turbidite sedimentary features. Microfossils are very rare. A few mica flakes and slate chips can be found in the hemipelagic mud.

3.1.33 Core 37 (335.9 - 344.27 mbsf) and Core 38 (345.6 - 354.72 mbsf)

Sedimentological features of Core 37 (Appendix Fig. 34) and Core 38 are similar (Appendix Fig. 35). There are several very fine sand to silt layers. Mica flakes can be found in the coarse fraction (> 250 μm) and foraminifers are always very rare.

3.1.34 Core 39 (355.30 - 363.27 mbsf)

Core 39 is predominated by hemipelagic mud (Appendix Fig. 36). In these fine sediments both benthic and planktic foraminifers are very rare (< 20 tests in 20 grams dry sediment), indicating a clear dilution effect due to a high sedimentation rate. Mica flakes are observed in several very fine sand to silt layers.

3.1.35 Core 40 (364.9 - 373.42 mbsf)

Core 40 consists predominantly of hemipelagic mud (Appendix Fig. 37). No turbidite structure is observed. Volcanic detritus can be found in core CC (37 - 42 cm), section 4 (39 - 44 cm) and 134 - 139 cm of section 2. Foraminifers are very rare (< 20 tests in 20 grams of dry sediment), but they are all indigenous fauna.

3.1.36 Core 41 (374.6 - 383. 37 mbsf)

Core 41 is composed of hemipelagic muds with rare very thin (< 0.1 cm), very fine sand to silt layers (Appendix Fig. 38). No turbidite structure can be observed. Volcanic detritus is found in the upper part (4 - 6 cm of section 1) of the core. Microfossils are very rare (< 10 tests in 20 grams of dry sediment).

3.1.37 Core 42 (384.2 - 392.95 mbsf)

Lithology of Core 42 (Appendix Fig. 38) and Core 41 (Appendix Fig. 39) is similar. However, foraminiferal tests in Core 42 are more abundant than in Core 41(> 100 tests/20 g of dry sediment). These benthic foraminifers are all indigenous deep-water species.

3.1.38 Core 43 (393.9 - 399.19 mbsf) and Core 44 (403.5 - 408.1 mbsf)

Both Core 43 (Appendix Fig. 40) and Core 44 (Appendix Fig. 41) are predominated by hemipelagic muds. Some mica and slate chips are found in the hemipelagic mud of both cores in which benthic foraminifers of well-preserved indigenous deep-marine species range from generally rare to common. No turbidite feature can be found.

3.2 Sand Layer Ratio

The Silt-Sand Layer Ratio (SLR) is defined as the ratio of the total thickness of silt-sand layers in each 1.5 m long section of core multiplied by 100%. The results are listed in Table 1 and shown as Fig. 2. Based on the SLR data, Hole 1202D can be divided into 8 sections: Section I (0 - 133 m, Cores 0-15) is almost barren of silt-sand layers (SLR < 5 %); Section II's (133 - 167. 95 m, Cores 16-19) SLR fluctuates between 3 and 7 %; Section III's (167.95 - 199.12 m, Cores 19-22) SLR increases to 45% in the upper part of Core 22; Section IV's (199.12 - 223.82 m, Core 22-25) SLR remains high (12 - 44 %; the highest SLR of 44.7 % is at the lower part of Core 25). Between Sections III and IV, there is a lower SLR interval; Section V (223.82 - 280.35 m, Cores 25-31) is characterized by a very high SLR (> 29 % with the highest SLR up to 90 - 100 % in Cores 27 and 28) and the lowest sediment recovery in Hole 1202D. The SLR then decreases gradually down core from a high peak in Section V through moderate SLR values (4 - 27 %) in Section VI (280.35 - 310.75 m, Cores 31-34) and Section VII (SLR: 4 - 10 %; 310.75 - 338.15 m in Cores 34-37) to a low SLR value (< 3 %) in Section VIII (338.15 - 407.24 m, Cores 37-44).

Using the age model constructed by Wei et al (2005), turbidite sand layer deposition in Hole 1202D is rare in the last 33 ka or Stages 1-2 and the upper part of Stage 3 (Fig. 2).

Table 1. Calculation of silt-sand layer ration (SLR) in Hole 1202D

core	section	interval (mbsf)		Silt-sand thickness (cm)	SLR (%)	Remarks
		top	bottom			
4	1	19.2	20.7	0	0.0	A
4	2	20.7	22.2	0.6	0.4	A
4	3	22.2	23.7	3.5	2.4	A
4	4	23.7	25.2	3.5	2.4	A
4	5	25.2	26.7	4.1	3.0	A
4	6	26.7	28.2	2.6	1.7	A
4	7	28.2	29.09	3.5	4.1	A
5	1	28.7	30.2	5.9	3.9	A
5	2	30.2	31.7	4.1	2.7	A
5	3	31.7	33.2	0	0.0	A
5	4	33.2	34.7	0.5	0.3	A
5	5	34.7	36.2	0.3	0.2	A
5	6	36.2	37.7	0.3	0.2	A
5	7	37.7	38.31	0.9	1.5	A
6	1	38.2	39.7	0.3	0.2	A
6	2	39.7	41.2	0.1	0.1	A
6	3	41.2	42.7	0.9	0.6	A
6	4	42.7	44.2	1.8	1.2	A
6	5	44.2	45.7	1	0.7	A
6	6	45.7	47.2	0	0.0	A
6	7	47.2	48.02	0.2	0.2	A
7	1	47.7	49.2	0.9	0.6	A
7	2	49.2	50.7	0.4	0.3	A
7	3	50.7	52.2	0.3	0.2	A
7	4	52.2	53.7	0.6	0.4	A

Table 1. Continued.

7	5	53.7	55.2	0.6	0.4	A
7	6	55.2	56.7	0.6	0.4	A
7	7	56.7	57.51	0	0.0	A
8	1	57.2	58.7	0.6	0.4	A
8	2	58.7	60.2	0.6	0.4	A
8	3	60.2	61.7	0.1	0.1	A
8	4	61.7	63.2	1	0.7	A
8	5	63.2	64.7	0.2	0.1	A
8	6	64.7	66.2	0.8	0.5	A
8	7	66.2	67.11	0	0.0	A
9	1	66.7	68.2	0	0.0	A
9	2	68.2	69.7	0	0.0	A
9	3	69.7	71.2	0	0.0	A
9	4	71.2	72.7	0	0.0	A
9	5	72.7	74.2	0	0.0	A
9	6	74.2	75.7	2.5	1.7	A
9	7	75.7	76.59	0.1	0.1	A
10	1	76.2	77.7	0.5	0.3	A
10	2	77.7	78.7	0	0.0	A
10	3	78.7	79.53	3	3.6	A
11	1	85.7	87.2	0	0.0	A
11	2	87.2	88.7	0.1	0.1	A
11	3	88.7	89.85	0	0.0	A
12	1	95.3	96.8	0	0.0	A
12	2	96.8	98.3	0	0.0	A
12	3	98.3	99.8	0	0.0	A
12	4	99.8	101.01	0	0.0	A

Table 1. Continued.

13	1	104.9	106.4	0.05	0.0	A
13	2	106.4	107.9	0	0.0	A
13	3	107.9	109.4	1.1	0.8	A
13	4	109.4	110.9	1.2	0.8	A
13	5	110.9	112.03	1	0.9	A
14	1	114.5	116	3	2.0	A
14	2	116	117.5	0.05	0.0	A
14	3	117.5	119	1.7	1.2	A
14	4	119	120.5	3.1	2.1	A
14	5	120.5	122	7.7	5.2	A
14	6	122	123.5	2.3	1.7	A
14	7	123.5	123.93	0.3	0.7	A
15	1	124.1	125.6	1.3	0.9	A
15	2	125.6	127.1	2.4	1.6	A
15	3	127.1	128.6	1.9	1.3	A
15	4	128.6	130.1	2.8	1.9	A
15	5	130.1	131.6	1.2	0.8	A
15	6	131.6	133.1	4.4	3.1	A
15	7	133.1	133.57	0.5	1.1	B
16	1	133.8	135.3	8.2	5.5	B
16	2	135.3	136.8	6	4.4	B
16	3	136.8	138.3	9.5	7.0	B
16	4	138.3	139.8	5	3.7	B
16	5	139.8	141.3	5.3	4.7	B
16	6	141.3	141.94	3.2	6.0	B
17	1	143.4	144.9	5.8	4.3	B
17	2	144.9	146.4	10.2	7.3	B

Table 1. Continued.

17	3	146.4	147.9	8.2	6.3	B
17	4	147.9	149.4	7	4.9	B
17	5	149.4	150.9	6.35	5.1	B
17	6	150.9	152	4.5	4.5	B
17	7	152	152.56	0.9	1.9	B
18	1	153	154.5	0.3	0.2	B
18	2	154.5	155.88	7.8	6.5	B
18	3	155.88	157.25	5.4	4.5	B
18	4	157.25	158.75	8.1	5.7	B
18	5	158.75	160.25	10.9	8.4	B
18	6	160.25	161.54	2.8	2.2	B
19	1	162.7	164.2	2	1.5	B
19	2	164.2	165.7	0.5	0.4	B
19	3	165.7	167.2	0.3	0.2	B
19	4	167.2	168.7	0.9	0.6	C
19	5	168.7	170.2	3.9	3.1	C
19	6	170.2	170.97	4.3	6.2	C
20	1	172.3	173.8	2.9	2.1	C
20	2	173.8	175.3	13.8	9.8	C
20	3	175.3	176.8	7.4	5.7	C
20	4	176.8	178.3	23.7	16.9	C
20	5	178.3	179.68	14.7	11.8	C
21	1	182	183.5	20.4	14.8	C
21	2	183.5	185	50.6	35.6	C
21	3	185	186.5	32.1	24.8	C
21	4	186.5	187.6	21.3	20.9	C
21	5	187.6	188.25	18.5	34.6	C

Table 1. Continued.

22	1	191.7	193.2	60.3	44.3	C
22	2	193.2	194.7	63.5	45.0	C
22	3	194.7	196.2	19.3	14.6	C
22	4	196.2	197.7	34.8	25.5	C
22	5	197.7	198.9	13	12.3	C
22	6	198.9	199.33	2.4	5.6	D
23	1	201.3	202.8	13.6	9.9	D
23	2	202.8	204.3	11.4	8.5	D
23	3	204.3	205.8	26.9	20.2	D
23	4	205.8	206.82	9.8	12.4	D
23	5	206.82	208.08	20.8	19.0	D
24	1	210.9	212.4	22.9	16.8	D
24	2	212.4	213.9	25	17.9	D
24	3	213.9	215.4	30.1	22.9	D
24	4	215.4	216.9	36.9	26.2	D
24	5	216.9	217.93	15	16.3	D
24	6	217.93	218.54	10.4	19.6	D
25	1	220.5	222	42.7	31.6	D
25	2	222	223.5	58.4	44.8	D
25	3	223.5	224.13	3.1	5.8	D
27	1	239.7	241.2	78.6	62.4	E
27	2	241.2	242.7	40.3	29.8	E
27	3	242.7	243.87	71.6	72.0	E
28	1	249.3	250.8	145.5	100.0	E
28	2	250.8	252.3	130.9	92.2	E
28	3	252.3	253.15	41.3	49.0	E
30	1	268.5	270	68.6	51.6	E

Table 1. Continued.

30	2	270	270.35	22	62.9	E
31	1	278.1	279.6	0	0.0	E
31	2	279.6	281.1	0	0.0	E
31	3	281.1	282.6	6.6	4.4	F
31	4	282.6	284.1	19	12.7	F
31	5	284.1	285.37	11.8	9.3	F
31	6	285.37	286	15.2	27.6	F
32	1	287.8	289.3	0.2	0.1	F
32	2	289.3	290.8	26.8	19.1	F
32	3	290.8	292.26	23.5	18.6	F
32	4	292.26	293.76	35.4	25.7	F
32	5	293.76	295.01	22.5	20.7	F
33	1	297.4	298.9	3.9	2.9	F
33	2	298.9	300.4	5.7	4.2	F
33	3	300.4	301.82	9.7	8.1	F
33	4	301.82	303.32	0.6	0.5	F
33	5	303.32	304.47	3.5	3.5	F
33	6	304.47	305.67	0.2	0.2	F
34	1	307	308.5	10.8	8.0	F
34	2	308.5	310	0.2	0.1	F
34	3	310	311.5	0	0.0	G
34	4	311.5	313	2.4	1.7	G
34	5	313	314.5	3.9	2.8	G
34	6	314.5	315.42	0.4	0.5	G
35	1	316.6	318.1	4.9	3.7	G
35	2	318.1	319.6	0.95	0.7	G
35	3	319.6	321.1	0.4	0.3	G

Table 1. Continued.

35	4	321.1	322.41	4.2	3.5	G
35	5	322.41	323.93	5.8	4.2	G
35	6	323.93	325.29	0.5	0.4	G
36	1	326.2	327.7	0.3	0.2	G
36	2	327.7	329.2	4.2	3.1	G
36	3	329.2	330.7	2.6	2.0	G
36	4	330.7	332.2	4.8	3.5	G
36	5	332.2	333.54	10.4	8.7	G
36	6	333.54	334.57	9.75	10.5	G
37	1	335.9	337.4	2.2	1.5	G
37	2	337.4	338.9	1.9	1.3	H
37	3	338.9	340.4	1.4	0.9	H
37	4	340.4	341.63	0.5	0.4	H
37	5	341.63	342.63	1.1	1.1	H
37	6	342.63	343.35	0.6	0.8	H
38	1	345.6	347.1	1.9	1.3	H
38	2	347.1	348.6	1.6	1.1	H
38	3	348.6	350.1	2.4	1.6	H
38	4	350.1	351.6	2	1.3	H
38	5	351.6	353.1	0.6	0.4	H
38	6	353.1	354.15	0.1	0.1	H
39	1	355.3	356.8	0.8	0.5	H
39	2	356.8	358.3	1.4	0.9	H
39	3	358.3	359.8	1.8	1.2	H
39	4	359.8	361.18	0.9	0.7	H
39	5	361.18	362.08	0.2	0.2	H
39	6	362.08	363.27	0.3	0.3	H

Table 1. Continued.

40	1	364.9	366.4	2.6	1.7	H
40	2	366.4	367.9	1.7	1.1	H
40	3	367.9	369.4	1.3	0.9	H
40	4	369.4	370.9	3.8	2.5	H
40	5	370.9	372.36	1.7	1.2	H
41	1	374.6	376.1	1.7	1.1	H
41	2	376.1	377.6	1.4	0.9	H
41	3	377.6	379.1	1.5	1.0	H
41	4	379.1	380.6	0.4	0.3	H
41	5	380.6	381.99	1.3	0.9	H
41	6	381.99	382.99	1	1.0	H
42	1	384.2	385.7	0.4	0.3	H
42	2	385.7	387.2	0.6	0.4	H
42	3	387.2	388.7	0.9	0.6	H
42	4	388.7	390.2	1.7	1.1	H
42	5	390.2	391.7	0.4	0.3	H
42	6	391.7	392.7	0.2	0.2	H
43	1	393.9	395.4	0.6	0.4	H
43	2	395.4	396.9	1.1	0.7	H
43	3	396.9	398.4	0.9	0.6	H
43	4	398.4	398.85	0.5	1.1	H
44	1	403.5	405	1.3	0.9	H
44	2	405	406.5	1	0.7	H
44	3	406.5	407.97	1.15	0.8	H

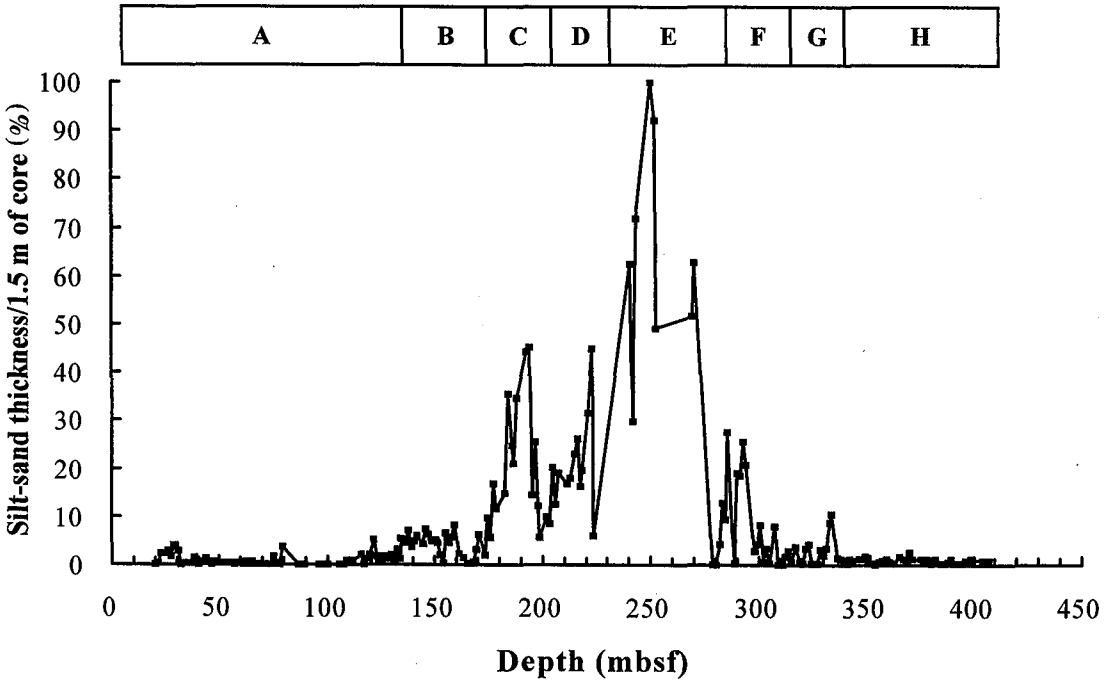

Fig. 2. Ratio of silt-sand layer thickness (SLR) in each 1.5 m length of core, Hole 1202D. Based on this SLR ratio, the core can be divided into 8 sections (A to H).

However, it became very common during Stages 3 and 4.

3.3 Composition of Detritus in the Coarse Fraction (> 250 μm)

Terrigenous detritus in washing residues (coarse fraction >250 μm) of Hole 1202D are determined under stereo-microscope (X60) and the results are listed in Table 2. Terrigenous detritus in Hole 1202D are primarily composed of slate chips, volcanics, mica flakes and quartz grains (Fig. 3). We put volcanic fragments and volcanic minerals with distinct crystal forms together as volcanics in Table 2. Both sedimentary and volcanic origins of quartz grains were found; however, it is difficult to identify them precisely under a stereo-microscope. Consequently they have been listed together in Table 2, and the significance is not considered. However, elimination of quartz grains ought not interfere with conclusions as to sediment sources as the remaining three components (slate, mica and volcanics) are all adequately represented to reflect sediment provenances. Slate fragments are commonly found in turbidite dominant intervals (160 - 280 m), while mica flakes can be found in fine sediments throughout the core. Volcanic detritus appear in the middle and lower parts of the core. Slate and mica are

frequently found in study samples, but volcanic detritus usually appear alone (Fig. 3). Occurrences of these major components of detritus suggest that the materials were primarily derived from the Central Range of Taiwan where the Miocene deep-marine slates of accretionary prism overlay the Early Tertiary - Paleozoic metamorphic basement of the underthrust Eurasian continent (Fig. 4) in northern Taiwan (Huang et al. 1977; 2000). Volcanics could represent eruptions in the active-extension back-arc basin of the southern Okinawa Trough off NE Taiwan or secondary erosions from the submarine volcanic mountains in the trough. The bathymetric map of the southern Okinawa Trough shows there are two submarine canyons (A and C in Fig. 1). Between these two submarine channels, there is a concave depression (B in Fig. 1) due to slope failure. The northern submarine canyon (A in Fig. 1) is active today and has a point-source following the onland Lanyang River which develops from the accretionary wedge slate belt in the western part of Central Range of northern Taiwan (Fig. 1). The southern submarine canyon (C in Fig. 1) does not have an active source today. The canyon C can be traced to the continental shelf (150 m in depth). Since there is no major river except the Lanyang River north of 24°30'N, the submarine canyon C could represent a paleo-channel of this river during the last glacial time before channel migration in the Holocene due to sea-level rise. Here, the sediments eroded from the Central Range were transported to the site of Hole 1202D either via submarine channel transportation or by slope failures before finally being deposited in the southern Okinawa Trough.

In addition, shallow-marine fossils including benthic foraminifers, echinoids, bryozoans and mollusks were also transported into deep-marine environments (Table 2). The fossil assemblages could have been deposited in shallow-shelf and then transported to the deep depositional site via submarine channel erosion or by slope failures due to frequent earthquakes induced by plate convergence/collision and extension of the southwestern Okinawa Trough off NE Taiwan (Kao et al. 1998; Huh et al. 2004).

4. CONCLUSIONS

The sediments of ODP Site 1202, Leg 195, in the southern Okinawa Trough consist of hemipelagic mud in the upper 100 m (Stages 1-2). Silt-sand layers occur from 133 mbsf (Stage 3) down core to 337 mbsf (Stage 4). The Silt-Sand Layer Ratio (SLR) increases from < 10 % in 133 - 167 m to more than 50 % in 223 - 279 m, then decreases to less than 10 % in 310 - 337 m and less than 3 % in 337 - 407 m (Stage 4), suggesting fine grained turbidite depositions were very active in Stages 3 and 4. Detritus in wash residues (> 250 μm) of Hole 1202D are predominated by slate fragments, quartz grains, mica flakes and volcanic detritus. Slate fragments, quartz grains and mica flakes are primarily derived from the accretionary prism of the Central Range in northern Taiwan where the Miocene slates overlay the Early Tertiary - Paleozoic schists and marbles of underthrust Eurasian continent. Occurrences of volcanics could represent submarine volcanic activity in the active-opening Okinawa Trough back-arc basin off NE Taiwan. Shallow-marine fossils including benthic foraminifers, echinoids, bryozoans and mollusks were also transported into deep-marine environments. The fossil assemblages could have been deposited in the shallow-shelf and then transported to the deep depositional site via

Table 2. Occurrence of detritus and bioclastics in coarse fraction (> 250 μm) of wash residues of Hole 1202D, Leg 195. X: barren; R: rare; A: Abundant.

core	section	Depth (mbsf)		volcanics	slates	metamorphics	total	Volcanics (%)	Slates (%)	Metamorphics (%)	Mollusks	Echinoderms	Spongy
012X	01W	96.55	96.6	0	11	5	16	0	68.8	31.3	X	X	X
014X	05W	121.19	121.26	14	7	56	77	18.2	9.1	72.7	A	X	A
016X	01W	134.81	134.84	0	27	0	27	0	100	0	X	X	X
016X	02W	135.7	135.73	0	84	10	94	0	89.4	10.6	A	R	R
016X	04W	138.93	138.97	3	8	7	18	16.7	44.4	38.9	R	X	X
016X	04W	139.55	139.6	0	32	10	42	0	76.2	23.8	A	A	A
016X	06W	141.7	141.74	0	46	3	49	0	93.9	6.1	X	X	X
017X	01W	144.4	144.44	338	483	6	827	40.9	58.4	0.7	X	X	X
017X	04W	148.01	148.06	0	43	7	50	0	86	14	A	A	X
017X	06W	151.54	151.58	64	1	0	65	98.5	1.5	0	X	X	X
018X	01W	154.13	154.18	0	8	0	8	0	100	0	X	X	X
018X	04W	158.63	158.67	3	3	13	19	15.8	15.8	68.4	A	A	A
018X	05W	159.53	159.55	6	310	13	329	1.8	94.2	4	R	R	R
020X	02W	174.21	174.25	11	0	14	25	44	0	56	A	A	A
020X	03W	176.55	176.6	0	8	36	44	0	18.2	81.8	R	X	X
020X	04W	177.8	177.85	0	18	46	64	0	28.1	71.9	A	A	A
021X	01W	182.21	182.26	0	17	2	19	0	89.5	10.5	A	A	X
021X	02W	183.88	183.93	5	48	15	68	7.4	70.6	22.1	X	X	X
021X	02W	184.49	184.54	0	125	14	139	0	89.9	10.1	X	X	X
021X	03W	186.03	186.08	0	0	59	59	0	0	100	X	R	R
021X	04W	186.95	186.97	0	0	12	12	0	0	100	X	X	X
021X	05W	187.73	187.76	0	1	135	136	0	0.7	99.3	X	R	X
022X	01W	192.65	192.68	24	10	9	43	55.8	23.3	20.9	A	A	A
022X	04W	196.52	196.56	0	0	14	14	0	0	100	X	X	X
023X	03W	205.55	205.6	0	1	83	84	0	1.2	98.8	A	A	A

Table 2. Continued.

023X	03W	205.7	205.75	0	69	22	91	0	75.8	24.2	A	A	X
023X	05W	207.9	207.92	45	41	0	86	52.3	47.7	0	A	X	X
024X	01W	212.04	212.08	42	3	0	45	93.3	6.7	0	R	X	X
024X	01W	212.13	212.15	4	17	58	79	5.1	21.5	73.4	X	X	R
024X	03W	215.03	215.06	6	29	1	36	16.7	80.6	2.8	R	X	X
024X	03W	215.07	215.09	92	198	37	327	28.1	60.6	11.3	X	X	X
024X	03W	215.15	215.2	2	8	6	16	12.5	50	37.5	R	X	R
024X	05W	217.64	217.67	122	247	0	369	33.1	66.9	0	A	A	X
025X	02W	222.63	222.66	41	0	8	49	83.7	0	16.3	X	X	X
026X	CCW	230.16	230.2	0	0	139	139	0	0	100	X	X	X
027X	01W	239.84	239.88	8	20	341	369	2.2	5.4	92.4	A	X	X
027X	01W	240.84	240.88	5	5	9	19	26.3	26.3	47.4	X	X	X
027X	02W	241.86	241.91	0	0	9	9	0	0	100	X	X	X
027X	03W	243.36	243.4	0	0	8	8	0	0	100	X	X	X
027X	03W	243.74	243.78	0	0	10	10	0	0	100	X	X	X
027X	03W	243.84	243.86	0	0	275	275	0	0	100	A	X	X
028X	02W	252.05	252.1	0	0	100	100	0	0	100	X	X	X
028X	03W	253	253.05	4	4	766	774	0.5	0.5	99	A	A	A
030X	01W	269.09	269.13	15	0	401	416	3.6	0	96.4	A	A	A
030X	02W	270.3	270.34	23	0	364	387	5.9	0	94.1	A	A	A
030X	CCW	270.43	270.49	7	0	876	883	0.8	0	99.2	R	X	X
031X	02W	280.4	280.45	6	0	20	26	23.1	0	76.9	R	X	R
031X	04W	283.3	283.35	13	0	127	140	9.3	0	90.7	R	R	R
031X	04W	283.4	283.45	232	18	1	251	92.4	7.2	0.4	A	R	X
031X	05W	284.25	284.25	2	0	9	11	18.2	0	81.8	X	R	X
031X	06W	285.61	285.64	606	1	12	619	97.9	0.2	1.9	A	A	X
031X	06W	285.64	285.7	121	6	201	328	36.9	1.8	61.3	A	R	A

Table 2. Continued.

031X	06W	285.91	285.96	364	0	4	368	98.9	0	1.1	X	X	X
032X	02W	290.32	290.36	1	0	27	28	3.6	0	96.4	X	X	X
032X	05W	293.83	293.88	19	0	34	53	35.8	0	64.2	X	X	X
032X	05W	294.9	294.94	221	0	9	230	96.1	0	3.9	R	X	X
032X	05W	294.94	294.97	38	0	78	116	32.8	0	67.2	X	X	X
033X	03W	301.03	301.07	49	1	75	125	39.2	0.8	60	X	X	X
034X	01W	307.65	307.68	0	0	132	132	0	0	100	X	X	X
034X	01W	308.14	308.15	0	0	8	8	0	0	100	X	R	R
034X	01W	308.15	308.18	0	0	5	5	0	0	100	X	X	X
034X	03W	311.05	311.09	299	0	0	299	100	0	0	X	R	R
034X	05W	314.33	314.35	0	0	25	25	0	0	100	X	R	X
035X	03W	319.92	319.96	56	3	31	90	62.2	3.3	34.4	R	R	R
035X	03W	320.85	320.9	1	1	12	14	7.1	7.1	85.7	X	X	R
035X	04W	321.77	321.79	264	0	0	264	100	0	0	X	X	X
035X	05W	322.87	322.91	79	0	3	82	96.3	0	3.7	X	X	X
040X	02W	367.74	367.79	21	0	1	22	95.5	0	4.5	X	X	X
040X	03W	368.32	368.44	4	1	0	5	80	20	0	X	X	X
040X	03W	368.53	368.58	9	1	1	11	81.8	9.1	9.1	X	X	X
040X	04W	369.79	369.84	1000	0	0	1000	100	0	0	X	X	X
041X	01W	374.64	374.7	297	2	2	301	98.7	0.7	0.7	X	X	X
041X	05W	381.57	381.62	15	0	35	50	30	0	70	X	X	X
042X	01W	385.55	385.6	10	0	2	12	83.3	0	16.7	X	X	X
042X	04W	389.57	389.65	0	3	1	4	0	75	25	X	X	X
043X	03W	397.6	397.65	0	0	8	8	0	0	100	X	X	X
044X	02W	405.99	406.06	1	0	4	5	20	0	80	X	X	X

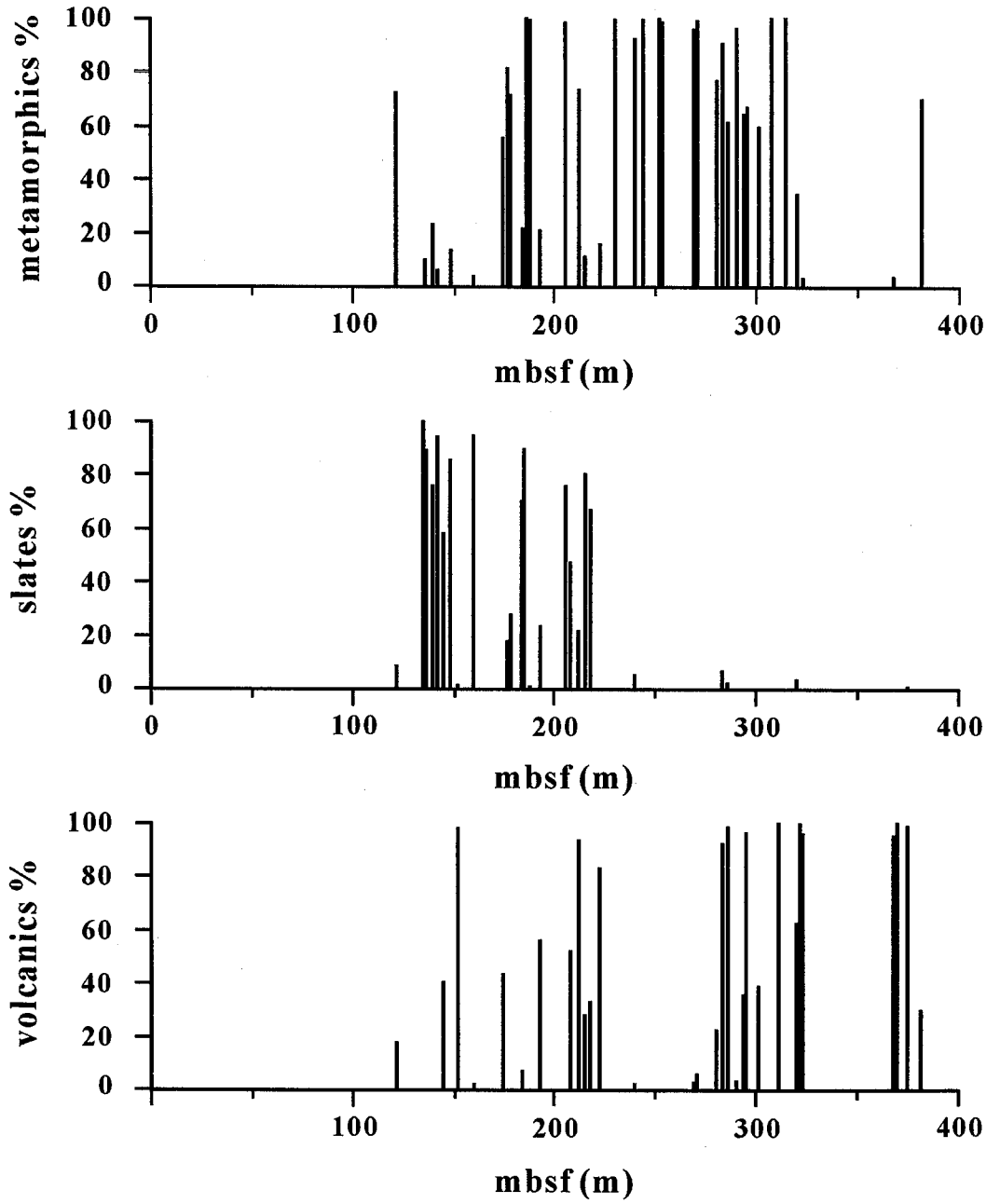

Fig. 3. Composition of volcanic, slate and metamorphic detritus in coarse fraction (> 250 μm) of Hole 1202D, Leg 195, in southern Okinawa Trough off NE Taiwan.

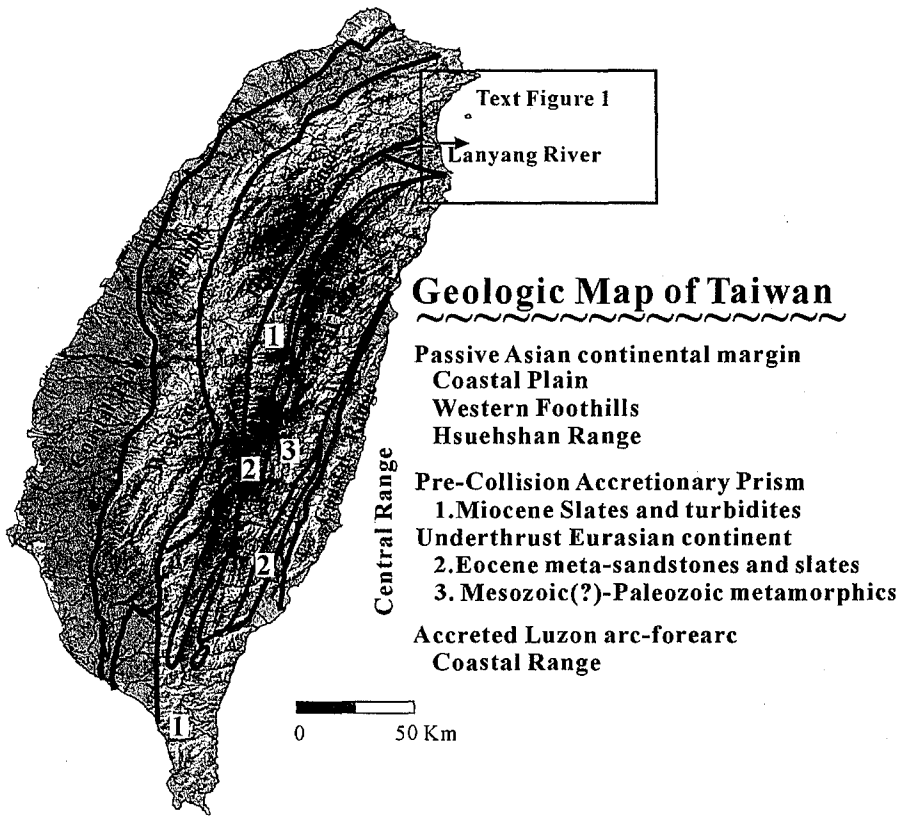

Fig. 4. General geology of Taiwan and location of the Lanyang River in NE Taiwan. The sediments in the southern Okinawa Trough were mostly derived from the Miocene slate belt of pre-collision accretionary prism in the western Central Range and the Early Tertiary-Paleozoic metamorphic basement of the underthrust Eurasian Continent in the eastern Central Range via the Lanyang River and its submarine channel.

submarine channel erosions or by the mass movement of slope failures due to frequent earthquakes induced by plate convergence/collision and extension of the southwestern Okinawa Trough off NE Taiwan.

Acknowledgements The authors appreciate Drs. Peter B. Yuan, B. R. Herbert, J. Baldauf, D. A. Brooks and B. Horan for their assistances in core description during the works in TAMU core laboratory and the Leg 195 Shipboard Scientific Party for drilling and documenting the

hole. This study was financially supported by NCKU-NSYSU Research Center of Ocean Environment and Technology, National Cheng Kung University, and grants from the National Science Council (NSC91-2116-M006-007; NSC92-2116-M006 -012), Taiwan, R.O.C..

REFERENCES

Chang, L. S., 1960: A biostratigraphic study of the Miocene in western Taiwan based on smaller foraminifera (Part II: Benthonics). *Bull. Geol. Surv. Taiwan.*, **12**, 67-91.

Huh, C. A., C. C. Su, W. T. Liang, and C. Y. Ling, 2004, Linkages between turbidites in the southern Okinawa Trough and submarine earthquakes. *Geophys. Res. Lett.*, **31**, L12304.

Huang, C. Y., W. Y. Wu, C. P. Chang, S. Tsao, P. B. Yuan, C. W. Lin, and K. Y. Xia, 1997: Evolution of the pre-collision accretionary prism in the arc-continent collision terrane of Taiwan. *Tectonophys.*, **281**, 31-51.

Huang, C. Y., P. B. Yuan, C. W. Lin, T. K. Wang., and C. P. Chang, 2000: Geodynamic processes of Taiwan arc-continent collision and comparison with analogs in Timor, Papua New Guinea, Urals, and Corsica. *Tectonophys.*, **325**, 1-21.

Liu, C. S., S. Y. Liu, S. E. Lallemand, N. Lundberg, and D. L. Reed, 1998: Digital elevation model offshore Taiwan and its tectonic implications. *Terr. Atmos. Ocean. Sci.*, **9**, 705-738.

Kao, H., S. S. Jack Shen, and K. F. Ma, 1998: Transition from oblique subduction to collision: Earthquakes in the southernmost Ryukyu-Taiwan region. *J. Geophys. Res.*, **103**, 7211-7229.

Wei, K. Y., H. S. Mii, and C. Y. Huang, 2005: Age Model and Oxygen Isotope Stratigraphy of Site ODP1202 in the Southern Okinawa Trough, Northwestern Pacific. *Terr. Atmos. Ocean. Sci.* **16**, 1-17.

Shipboard Scientific Party, Site 1202, 2002: In Salisbury, M.H., Shinohara, M., Richter, C., et al., Proc. Init. Repts., 195 1-46 (CD-ROM), Avaiable from: Ocean Drilling Program, Texas A&M Univ., College Station, TX 77845-9547, USA.

Zhao, M., C. Y. Huang, and K. Y. Wei, 2005: A 28000 Year Sea-Surface Temperature Record of ODP Site 1202B, the Southern Okinawa Trough. *Terr. Atmos. Ocean. Sci.* **16**, 45-56.

* Appendix is posted in the TAO Electronic Supplement at the TAO website (http://tao.cgu.org.tw)